

Article

Liberation of Adsorbed and Co-Precipitated Arsenic from Jarosite, Schwertmannite, Ferrihydrite, and Goethite in Seawater

Rodrigo Alarcón ^{1,*}, Jenny Gaviria ² and Bernhard Dold ^{1,2,3}

¹ Geology Department, University of Chile, Plaza Ercilla #803, Casilla 13518, Correo 21, Santiago 8320000, Chile

² Institute of Applied Economic Geology (GEA), University of Concepcion, Casilla 160-C, Concepción 4030000, Chile; E-Mail: jennygaviria@gmail.com

³ Present Address: SUMIRCO (Sustainable Mining Research & Consult EIRL), Casilla 28, San Pedro de la Paz 4130000, Chile; E-Mail: bernhard.dold@gmail.com

* Author to whom correspondence should be addressed; E-Mail: rodalarc@ing.uchile.cl; Tel.: +56-9-6678-9689.

Received: 10 March 2014; in revised form: 17 June 2014 / Accepted: 18 June 2014 /

Published: 8 July 2014

Abstract: Sea level rise is able to change the geochemical conditions in coastal systems. In these environments, transport of contaminants can be controlled by the stability and adsorption capacity of iron oxides. The behavior of adsorbed and co-precipitated arsenic in jarosite, schwertmannite, ferrihydrite, and goethite in sea water (common secondary minerals in coastal tailings) was investigated. The aim of the investigation was to establish As retention and transport under a marine flood scenario, which may occur due to climate change. Natural and synthetic minerals with co-precipitated and adsorbed As were contacted with seawater for 25 days. During this period As, Fe, Cl, SO₄, and pH levels were constantly measured. The larger retention capability of samples with co-precipitated As, in relation with adsorbed As samples, reflects the different kinetics between diffusion, dissolution, and surface exchange processes. Ferrihydrite and schwertmannite showed good results in retaining arsenic, although schwertmannite holding capacity was enhanced due its buffering capacity, which prevented reductive dissolution throughout the experiment. Arsenic desorption from goethite could be understood in terms of ion exchange between oxides and electrolytes, due to the charge difference generated by a low point-of-zero-charge and the change in stability of surface complexes between synthesis conditions and natural media.

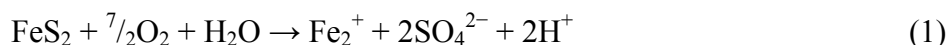
Keywords: arsenic; desorption; marine; coastal mine tailings; climate change; pollution; ferrihydrite; schwertmannite; mobility; environment; mining

1. Introduction

Arsenic is one of the most toxic inorganic pollutants in aquatic systems [1]. Its source is mainly geogenic, entering the environment through volcanic emissions, hydrothermal systems [2], mineral erosion, or by reductive dissolution of iron hydroxides, such as in the case of Bangladesh [3]. Although the input from anthropogenic sources (mining, fossil fuels) is lower than natural sources, these can have a strong impact, generating local pollution episodes [2]. There are mainly three mechanisms that explain arsenic liberation into natural environments [4]: (1) oxidation of arsenic sulphides, (2) competitive desorption, and (3) reductive dissolution of iron oxides. Although each has been extensively investigated under several experimental conditions, there is still a lack of knowledge as to how these processes take place in specific environments.

Some climatic models predict that, by the end of the century, one of the consequences of global warming will be a sea level rise of up to 1.1 m above the current level [5]. This sea level change will establish a new geochemical context in the oxidation zone of mine tailings and acid sulphate soils near the shoreline, where the stability of sorbent minerals under seawater flood would be uncertain. In this paper, the effects of seawater intrusion on arsenic adsorbed to or co-precipitated with major sorbent minerals, present in acid soils or mine tailings, are simulated. Synthesized jarosite, schwertmannite, goethite, and ferrihydrite were used to represent different arsenic uptake scenarios. The aim of these experiments is to establish the stability and transport of this metalloid in these coastal environments under changing environmental conditions.

Iron oxides behave as excellent sorbents for a variety of contaminants in almost every environment. They have been widely used in the extraction of heavy metals from natural [6] and industrial sources [7], which has generated a great number of studies about mechanisms of surface interactions [8–12]. These minerals are common in environments with high availability of metal sulphides exposed to oxidizing conditions, as in acid sulphate soils, in the oxidation zone of mine tailings, or ore deposits [13,14]. In these systems, oxidation of the primary sulphide (pyrite) is capable of releasing large amounts of protons, sulphate, Fe(II), and trace metals (Equation (1)) [15]. Once Fe(III) is produced by oxidation of Fe(II), which may be strongly accelerated by microbial activity under low pH conditions, Fe(III) becomes the primary oxidant of pyrite [16].



At circumneutral pH, ferrihydrite ($5\text{Fe}_2\text{O}_3 \cdot 9(\text{H}_2\text{O})$) is commonly the first mineral phase to precipitate from hydrolysis of ferric solutions [17]. Ferrihydrite is able to transform into crystalline phases of higher thermodynamic stability as goethite ($\alpha\text{-FeOOH}$) or hematite (Fe_2O_3) [18]. When the pH of the system is acidic enough (pH 2–4) and there is a high sulphate concentration, jarosite ($(\text{Na}, \text{K}, \text{H}_3\text{O}) \cdot [\text{Fe}_3(\text{SO}_4)_2(\text{OH})_6]$) (pH ~ 2) and schwertmannite ($\text{Fe}_{16}\text{O}_{16}(\text{OH})_{12} \cdot (\text{SO}_4)_2$) constitute the

main phases [13]. Between pH 2.5 and 4, schwertmannite is, perhaps, the principal secondary mineral that forms from acid drainage [19,20].

In natural environments, redox processes commonly control the solubility of iron oxides. This occurs when interaction occurs between dissolved species, such as H^+ , OH^- or other metal ions, with the hydroxyl groups present on the oxides surfaces [21,22]. Adsorption and formation of surface complexes with reducing species is a reaction that generates an electron transfer, reducing Fe(III) to Fe(II) [21]. Weaker Fe(II) bonds enhance reductive dissolution and release of species from oxides surfaces. For example, in Alberta (Canada) microbial activity in acid sulphate soils released significant amounts of As when the Eh was below +100 mV [23]. Mine tailings at the former Delnite gold mine in Northern Ontario showed that As(V) reduction and mobilization occurred due to reductive dissolution of goethite, influenced by a biosolid-cover [24]. Reductive dissolution also takes place in remediated marine shore tailings deposits [14]. Iron oxides under reductive conditions formed a Fe-Mn plume, which developed toward the shoreline where oxidizing and higher pH conditions triggered Fe(III) oxide-hydroxide precipitation.

When arsenic is present during hydrolysis of Fe(III) it can co-precipitate. In some minerals it can form part of the structure, for instance in jarosite at the TO_4 site [25,26], or it can be adsorbed as surface complexes [27]. In relation to iron oxides, arsenate tends to be adsorbed as outer-sphere complexes [28], while arsenite can be adsorbed either as inner or outer-sphere complexes [28,29].

Different studies using Extended X-ray Absorption Fine Structure (EXAFS) and Fourier transform infrared spectroscopy (FTIR) have attempted to establish the possible bond between arsenic and iron oxide surfaces without reaching consensus to date. Waychunas *et al.* [30] stated that, due to thermodynamic constraints, there is only a low chance for the formation of mononuclear monodentate and bidentate complexes. Some authors established that bidentate binuclear complexes are most likely to form due to their higher thermodynamic stability [31–33]. MICRO-EXAFS spectra of individual Fe(III) oxy-hydroxide grains point to inner-sphere bidentate-binuclear forms as the predominant As(V) complex and the existence of a second sphere corresponding mainly to bidentate-mononuclear [34]. Furthermore, other authors postulate that As complexes at the surface of goethite would be exclusively monodentate complexes [35] and when the As load increases significantly or pH level is greater than 6, then, only bidentate binuclear complexes are formed [30,33,36].

Some species can compete with As for available vacancies restricting the metalloid adsorption. Studies on ferrihydrite indicate that the extent of adsorption can be affected by ionic competition, mainly by $PO_4 \gg$ organic ligands $> SO_4 > Cl$ [37,38]. When As is part of the structure of iron oxides, the long term release is controlled by media dissolution, pH-dependent sorption/desorption, ion exchange, and transformation processes [27,39].

Tailings disposal in bays and beaches has been a widely used practice in the past and is still performed in places like Papua New Guinea and Indonesia [40]. Lihir gold mine on Niolam Island in Papua New Guinea annually produces over 35 Mt of waste rock which are dumped into nearshore deepwater valleys, and about 100,000 ML of post-processing tailings slurry deposited at depth from a sub-surface pipeline [41]. By representing a potential risk to marine ecosystems, one of the main challenges in this field is to determine the geochemical stability and pollution potential of tailings in flooded environments [42].

In Chañaral (Chile) about 220 Mt of tailings fill the homonymous bay covering an area of about 4 km². Dold [43] indicated the presence of an oxidation zone (>1 m) with significant amounts of arsenic associated with secondary Fe(III) oxide-hydroxides and jarosite. The instability of the sorbent phases and the intrusion of seawater, a product of variations within the coastal cycle, promoted the release of dissolved As, Mo, and colloidal adsorbed Cu and Zn into the ocean, generating an impact over the meiofaunal assemblages through increasing the bioavailability of heavy metals [44] and there has been no sign of recovery 35 years after ceasing disposal [45]. During the summer, high rates of evaporation promote capillary transport of Cu and Zn, which precipitate as efflorescent salts on the tailings surface, increasing the risk of metal exposure for the local community [43,46]. Remediation experiences of similar systems have been successfully implemented in environments where the hydrological characteristics allowed it (e.g., Bahia de Ite, Peru [14]).

Concentrations of arsenic in open ocean seawater usually do not exceed 2 µg/L [47]. It is found mainly as arsenate (As (V)), although, concentration of arsenite (As(III)) in coastal waters affected by anthropogenic activity can be as high as 19% of As_{Total} [48]. Arsenic in oxidizing environments can be mainly found as protonated species of AsO₄³⁻. Biological activity plays an important role in marine arsenic speciation, reducing arsenate to arsenite, given the low thermodynamic stability of arsenite in oxidizing environments (As(III)/As(V) ≈ 10⁻²⁶) [49]. It also plays a role in the formation of monomethylarsenic acid and dimethylarsenic acid; however, the concentration of this arsenic species is much smaller than the inorganic forms.

Low concentrations of organic matter present in seawater (1–3 mg/L CH₃O [50]) do not allow reductive dissolution to be an effective mechanism for As release, though in coastal environments organic matter is usually more abundant than that found in the open ocean, which could be an important factor in speciation and solubility of iron [51].

Although As(III) species are mainly limited by biological processes, As(III) can be found in large quantities in polluted mining areas, especially in reducing groundwater environments [48]; however, it was not considered for the purpose of this study.

2. Materials and Methods

Sorbent minerals used for this experiment were synthesized according to several procedures [13,17,52–57]. No sample of schwertmannite with co-precipitated arsenic was synthesized, instead, a natural sample from the acid mine drainage of Monte Romero mine (Iberian Pyrite Belt, Spain) was used [58]. Incorporation of arsenic was considered to be by surface adsorption and co-precipitation. Every mineral was characterized using a Rigaku RADII-C X-ray diffractometer (XRD) (35 kV, 15 mA) from 20° to 100° 2θ using a range of 0.05° 2θ and a counting time of 10 s per step. X-ray diffraction patterns confirmed the correct synthesis for the procedures used and are presented in Figures 1 and 2. Further information about the experimental procedure can be found in the supplementary information section. In order to simulate As release from Fe(III) oxide-hydroxides and jarosite during seawater intrusion, the synthesized minerals were contacted with seawater during a 25-day period.

Figure 1. X-ray diffraction pattern for jarosite (jt), goethite (gt), schwertmannite (sh), and ferrihydrite (fh).

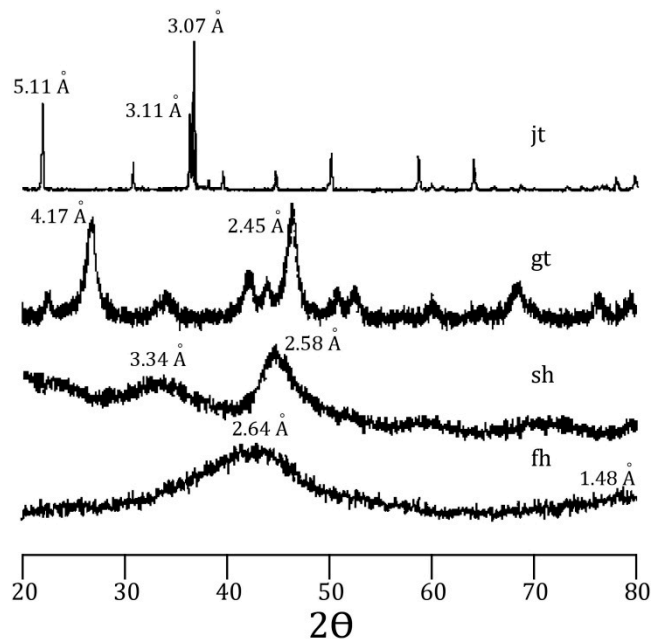
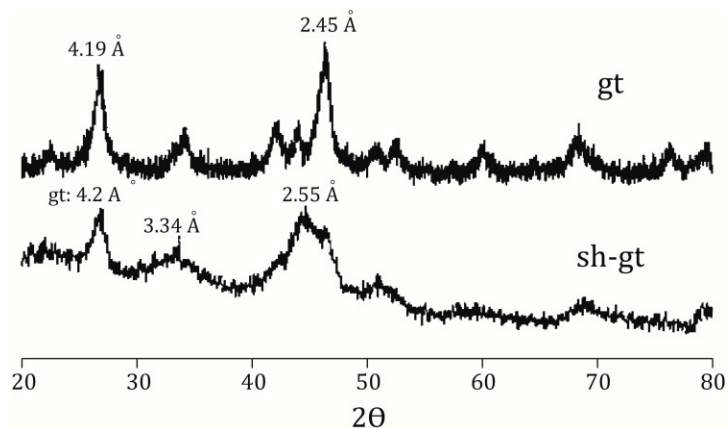


Figure 2. X-ray diffraction pattern for goethite (gt) and schwertmannite (sh-gt) with adsorbed As.



Twenty-five liters of seawater were taken 10 km offshore Concepción, Chile, by a research vessel. The chemical analysis of the seawater was carried out using titration methods with AgNO_3 for Cl^- and turbidimetry for SO_4^{2-} . As and Fe were both measured using an atomic absorption spectrometer (AAS), model Hitachi Z-8100 Polarized Zeeman (Hitachi, Tokyo, Japan). For the Fe analysis, Chelex-100 resin was used to pre-concentrate the sample with HNO_3 , which was then flushed to 10 mL. Arsenic hydrides were generated in the presence of H_2SO_4 , HNO_3 , and HClO_4 which were later used for readings (Tables 1 and 2). The respective detection limits were $5 \mu\text{g/L}$ for Fe and $1 \mu\text{g/L}$ for As.

Adsorbed and co-precipitated arsenic, associated with mineral samples, was measured using the same instrumental techniques as for sea water but with different acids for liberating the arsenic. Arsenic was detected in all samples as concentrations were above the detection limit. For every mineral used in this experiment, 1.5 g of the synthesized material (natural schwertmannite for co-precipitated As) was brought into contact with 400 mL of seawater in sealed vessels for 596 h

(~25 days). During this period, continuous stirring was applied (Figure 3). Over the duration of the experiments, 14 extractions (15 mL each) were taken, of which about 40% took place within the first 24 h. This was decided in order to track the period with the greatest release kinetics [59]. Every extraction was filtered using a 0.45 μm membrane filter, acidified with 50 μL of HNO_3 and stored at 4 $^\circ\text{C}$ until analysis. Concentrations of the released species are available in Tables 3–6. One of the limitations of this study is that pH and extractions were made at different times so there is some uncertainty regarding the correlation of these variables. However, long term trends, indicative of their relative behavior, can be identified in the figures and Table 7. All analyses were conducted in GEA Facilities (Instituto de Geología Económica Aplicada, Universidad de Concepción, Chile). In this work, computations involving arsenic and surface speciation were performed using PhreePlot [60]. Thermodynamic constants were taken from the wateq4f database. For the modeling of surface speciation, a charge distribution multisite ion complexation (CDMUSIC) model was chosen.

Table 1. Composition of sea water used in this study and comparison with literature values.

Ions/Metals	This work	Nordstrom [61]	Turekian [62]
Cl (g/L)	19.5	19.35	19.4
SO ₄ (g/L)	2.6	2.71	2.58
As ($\mu\text{g/L}$)	1	-	2.6
Fe (mg/L)	<0.008	0.002	0.0034

Table 2. Arsenic load in minerals used for this study.

Mineral		As (wt %)	As(mol/g)	As (mg/kg)
Schwertmannite	Co-precipitated	0.56	7.47×10^{-5}	21
	Adsorbed	0.81	1.08×10^{-4}	30.375
Ferrihydrite	Co-precipitated	2.97	3.96×10^{-4}	111.375
	Adsorbed	2.96	3.95×10^{-4}	111
Jarosite	Co-precipitated	0.16	2.14×10^{-5}	6
	Adsorbed	0.38	5.07×10^{-5}	14.25
Goethite	Co-precipitated	0.71	9.48×10^{-5}	26.625
	Adsorbed	3.34	4.46×10^{-4}	125.25

Figure 3. Magnetic stirrer with vessels containing schwertmannite samples.



Table 3. As release from ferrihydrite.

Experiment type	Without As				Co-precipitated As				Adsorbed As			
	Cl (g/L)	SO ₄ (g/L)	Fe (mg/L)	As (µg/L)	Cl (g/L)	SO ₄ (g/L)	Fe (mg/L)	As (µg/L)	Cl (g/L)	SO ₄ (g/L)	Fe (mg/L)	As (µg/L)
10	19.78	2.46	<0.05	<1	19.92	2.37	<0.05	253	19.62	1.53	<0.05	1227
10	19.45	2.33	<0.05	<1	19.43	2.49	<0.05	260	19.36	2.48	<0.05	1556
11	19.73	2.25	<0.05	<1	19.55	2.36	<0.05	260	19.72	2.29	<0.05	1533
13	19.55	2.35	<0.05	<1	19.94	2.36	<0.05	258	19.73	2.30	<0.05	1366
17	19.41	2.45	<0.05	<1	19.65	2.24	<0.05	263	19.80	2.25	<0.05	1254
23	21.74	2.39	<0.05	5	19.37	2.47	<0.05	224	19.63	2.47	<0.05	1088
36	20.65	2.35	<0.05	2	19.08	2.31	<0.05	226	19.44	2.26	<0.05	950
56	19.56	2.22	<0.05	2	19.09	2.06	<0.05	217	19.58	2.28	<0.05	849
85	19.45	2.63	<0.05	8	19.63	2.57	<0.05	189	18.93	2.51	<0.05	836
119	19.46	2.32	<0.05	-	19.12	2.17	<0.05	188	19.39	2.46	<0.05	692
180	19.50	2.24	<0.05	<1	19.50	2.63	<0.05	173	19.50	2.44	<0.05	693
260	19.50	2.39	<0.05	<1	19.50	2.34	<0.05	178	19.50	2.55	<0.05	682
416	19.50	2.14	<0.05	<1	19.50	2.75	<0.05	118	19.50	2.11	<0.05	308
596	19.50	2.43	<0.05	<1	19.50	2.72	<0.05	76	19.50	2.34	<0.05	273

Table 4. As release from schwertmannite.

Experiment type	Without As				Co-precipitated As				Adsorbed As			
	Cl (g/L)	SO ₄ (g/L)	Fe (mg/L)	As (µg/L)	Cl (g/L)	SO ₄ (g/L)	Fe (mg/L)	As (µg/L)	Cl (g/L)	SO ₄ (g/L)	Fe (mg/L)	As (µg/L)
10	19.73	2.31	<0.05	<1	21.29	2.50	<0.05	<1	19.64	2.65	<0.05	<1
10	19.51	2.76	<0.05	<1	20.00	2.40	<0.05	<1	20.28	2.42	<0.05	<1
11	19.73	2.62	<0.05	<1	19.68	2.27	<0.05	2	19.94	2.52	<0.05	<1
13	19.92	2.38	<0.05	<1	18.93	2.43	<0.05	<1	19.12	2.48	<0.05	<1
17	19.35	2.52	<0.05	<1	19.21	2.38	<0.05	<1	18.96	2.40	<0.05	3
23	19.09	2.70	<0.05	<1	19.05	2.64	0.42	9	19.16	2.43	<0.05	2
36	19.15	2.56	<0.05	<1	18.96	2.45	0.14	2	20.30	2.50	0.96	7
56	19.23	2.55	0.16	<1	19.13	2.49	0.17	<1	19.10	2.77	<0.05	1
85	19.33	2.54	0.24	<1	19.15	2.69	0.18	1	19.22	2.21	<0.05	2
119	19.99	2.24	0.20	1	19.36	2.51	0.27	<1	19.03	2.69	<0.05	2
180	19.50	2.64	0.20	<1	19.50	2.93	0.26	1	19.50	2.76	<0.05	3
260	19.50	2.68	0.26	7	19.50	2.75	0.29	2	19.50	2.70	<0.05	2
416	19.50	2.49	0.20	2	19.50	2.29	0.33	3	19.50	2.20	<0.05	2
596	19.50	2.35	0.10	2	19.50	2.39	0.42	2	19.50	2.32	<0.05	1

Table 5. As release from goethite.

Experiment type	Without As				Co-precipitated As				Adsorbed As			
	Cl (g/L)	SO ₄ (g/L)	Fe (mg/L)	As (µg/L)	Cl (g/L)	SO ₄ (g/L)	Fe (mg/L)	As (µg/L)	Cl (g/L)	SO ₄ (g/L)	Fe (mg/L)	As (µg/L)
10	19.54	2.38	<0.05	<1	18.97	2.97	<0.05	54	19.63	2.20	<0.05	6,572
10	19.44	2.37	<0.05	<1	19.59	2.47	<0.05	54	19.87	2.41	<0.05	9,378
11	19.44	2.14	<0.05	<1	19.54	2.35	<0.05	53	19.60	2.19	<0.05	15,404
13	19.30	2.35	<0.05	<1	19.44	2.62	<0.05	51	19.25	2.39	<0.05	19,721
17	20.28	2.20	<0.05	<1	19.44	2.48	<0.05	47	19.28	2.44	<0.05	20,620
23	19.27	2.20	<0.05	<1	19.39	3.19	<0.05	48	19.25	2.43	<0.05	25,776
36	19.35	2.14	<0.05	<1	19.97	2.48	<0.05	48	19.53	2.03	<0.05	24,873
56	19.33	2.19	<0.05	<1	19.71	2.18	<0.05	50	19.99	2.42	<0.05	22,994
85	19.33	2.29	<0.05	<1	19.65	2.37	<0.05	48	19.19	2.20	<0.05	24,000
119	19.71	2.51	<0.05	1	19.09	2.27	<0.05	50	19.40	2.52	<0.05	21,834
180	19.50	2.69	<0.05	3	19.50	2.53	0.14	50	19.50	2.77	0.08	22,776
260	19.50	2.62	<0.05	6	19.50	2.60	0.14	43	19.50	2.57	<0.05	19,578
416	19.50	2.07	0.08	1	19.50	2.26	0.08	34	19.50	2.26	<0.05	15,627
596	19.50	2.34	0.20	2	19.50	2.22	0.09	27	19.50	2.56	1.19	13,043

Table 6. As release from jarosite.

Experiment type	Without As				Co-precipitated As				Adsorbed As			
	Cl (g/L)	SO ₄ (g/L)	Fe (mg/L)	As (µg/L)	Cl (g/L)	SO ₄ (g/L)	Fe (mg/L)	As (µg/L)	Cl (g/L)	SO ₄ (g/L)	Fe (mg/L)	As (µg/L)
10	19.63	2.68	<0.05	<1	19.80	1.84	<0.05	4	19.93	2.18	<0.05	261
10	19.36	2.44	<0.05	<1	19.77	2.60	<0.05	6	19.64	2.31	<0.05	362
11	19.34	2.19	<0.05	<1	19.66	2.70	<0.05	5	19.23	2.39	<0.05	441
13	19.43	2.27	<0.05	<1	19.68	2.52	<0.05	7	19.42	2.46	<0.05	532
17	19.69	2.40	<0.05	<1	19.45	2.46	<0.05	7	19.68	2.43	<0.05	744
23	19.67	2.56	<0.05	<1	19.34	2.40	<0.05	7	19.79	2.48	<0.05	1000
36	19.35	2.39	<0.05	<1	19.24	2.61	<0.05	5	19.45	2.43	<0.05	1037
56	19.35	2.37	<0.05	5	19.29	2.54	<0.05	5	19.34	2.45	<0.05	1607
85	19.58	2.33	<0.05	<1	19.26	2.45	<0.05	5	19.21	2.52	<0.05	1799
119	19.68	2.72	<0.05	<1	19.36	2.55	<0.05	5	19.28	2.31	<0.05	1654
180	19.50	2.56	<0.05	2	19.50	2.80	<0.05	9	19.50	2.46	<0.05	2101
260	19.50	2.70	<0.05	<1	19.50	2.78	<0.05	7	19.50	2.74	0.49	2968
416	19.50	2.17	<0.05	<1	19.50	2.38	<0.05	5	19.50	2.27	3.02	6452
596	19.50	2.32	<0.05	1	19.50	2.55	<0.05	2	19.50	2.52	<0.05	4758

Table 7. pH during seawater saturation.

Ferrihydrite														
Without As	Hours	0	24	48	72	120	168	192	336	504	648			
	pH	7.2	6.4	7.7	8.0	7.7	7.7	7.3	7.9	7.3	7.4			
Co-precipitated As	Hours	0	24	48	72	120	168	192	336	504	648			
	pH	7.2	6.5	7.7	8.0	7.7	7.8	7.6	7.9	7.5	7.3			
Adsorbed As	Hours	0	24	48	96	144	168	312	480	648				
	pH	7.2	7.7	8.0	7.8	7.9	7.7	7.9	7.5	7.5				
Schwertmannite														
Without As	Hours	0	24	72	96	120	192	216	240	288	336	360	504	672
	pH	7.2	5.2	3.6	3.3	3.6	3.6	3.6	3.6	3.6	3.6	3.6	3.5	3.5
Co-precipitated As	Hours	0	48	72	96	168	192	216	264	312	336	480	648	
	pH	7.2	4.6	3.6	3.9	3.7	3.9	3.8	3.8	3.8	3.8	3.7	3.7	3.5
Adsorbed As	Hours	0	24	48	96	144	168	312	480	648				
	pH	7.2	4.0	4.3	4.2	4.2	4.2	4.2	4.1	4.1				
Jarosite														
Without As	Hours	0	24	72	96	120	192	216	240	288	336	360	504	672
	pH	7.2	7.9	6.9	8.0	8.0	6.8	7.6	7.9	7.8	7.6	7.4	5.4	5.9
Co-precipitated As	Hours	0	48	72	96	168	192	216	264	312	336	480	648	
	pH	7.2	8.0	8.3	8.2	6.9	7.3	7.9	7.9	7.7	7.7	7.5	7.0	
Adsorbed As	Hours	0	24	48	96	144	168	312	480	648				
	pH	7.2	7.6	8.0	8.0	7.9	7.8	7.7	7.6	7.5				
Goethite														
Without As	Hours	0	24	72	96	120	192	216	240	288	336	360	504	672
	pH	7.2	6.8	5.7	8.2	8.1	7.2	6.8	8.0	7.7	7.7	7.7	7.8	7.3
Co-precipitated As	Hours	0	48	72	96	168	192	216	264	312	336	480	648	
	pH	7.2	8.0	8.2	8.1	7.1	6.7	8.0	7.8	7.8	7.7	7.9	7.7	
Adsorbed As	Hours	0	24	48	96	144	168	312	480	648				
	pH	7.2	7.3	8.1	8.0	8.0	7.9	8.2	7.8	7.7				

3. Results and Discussion

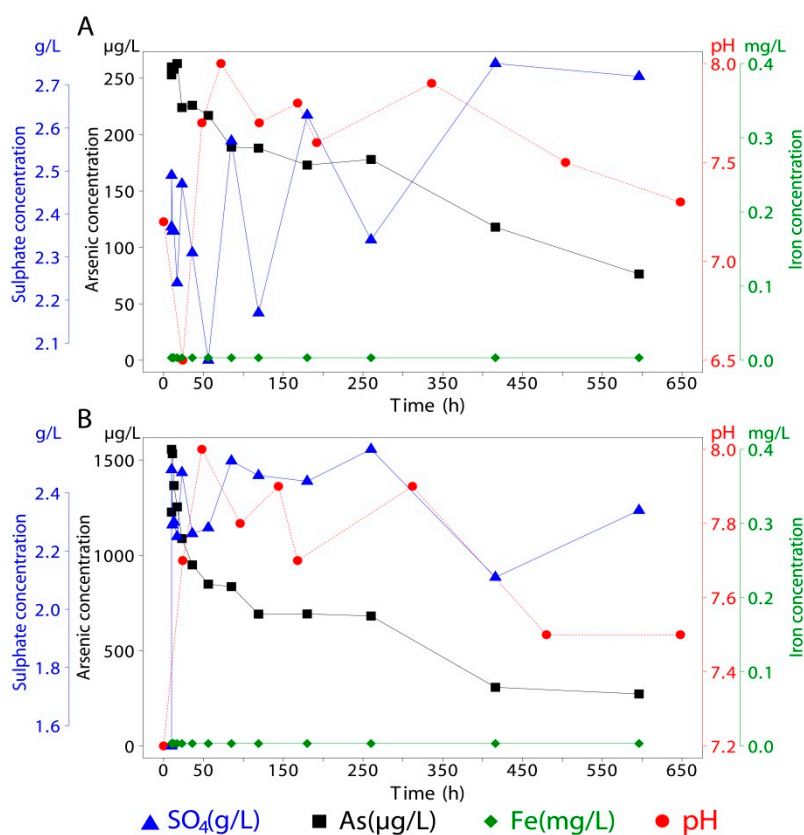
3.1. Arsenic Release from Ferrihydrite

The highest rate of liberation from ferrihydrite with co-precipitated arsenic occurred within the first 20 h, with a maximum of 260 µg/L. This corresponds to approximately 0.2% of the total load capacity (TLC) for this synthesis. After that, a decrease in dissolved arsenic showed two main steps until reaching 76 µg/L after 25 days from the beginning of the experiment (Figure 4; Table 3). The pH strongly decreased during the first 24 h; however, this did not show any relationship to Fe concentrations, which always remained below detection limit. It is possible that, during arsenic co-precipitation, a small fraction of the metalloid could be adsorbed as surface complexes, in which case the initial release could be related to ion exchange rather than dissolution.

Ferrihydrite with adsorbed As instantly reacted with seawater, releasing about 1.4% TLC (1555 µg/L) within 10 h, followed by a reduction to 273 µg/L towards the end of the experiment (Figure 4). The pH remained stable around 7.5 and no Fe release was measured. This was expected at neutral pH, with

concentrations of OH^- and H^+ being inadequate to promote dissolution [18]. The high load capacity for synthetic ferrihydrite (2.96 wt %) could be explained in terms of surface area, which for this mineral can reach up to $600 \text{ m}^2/\text{g}$ (Table S1 in supplementary information) and enables ferrihydrite to better react with the surrounding media. Under this scenario, stability of inner-sphere bidentate complexes [30] at the given conditions would be responsible for high arsenic retention. Nevertheless, Jain [63] determined that adsorbed As(V) in ferrihydrite can cause a reduction of the point of zero charge (PZC), by as much as 2.4 pH units.

Figure 4. Arsenic release from ferrihydrite. (A) Arsenic release from co-precipitated ferrihydrite and (B) arsenic release from adsorbed ferrihydrite.



This could be what triggers limited desorption by ion exchange in this case, due to the difference in electric charge between the electrolyte and ferrihydrite PZC (Table S2). Ferrihydrite transformation to goethite should not affect the results of this study ($\sim 1\%$ transformed after 500 h [64]).

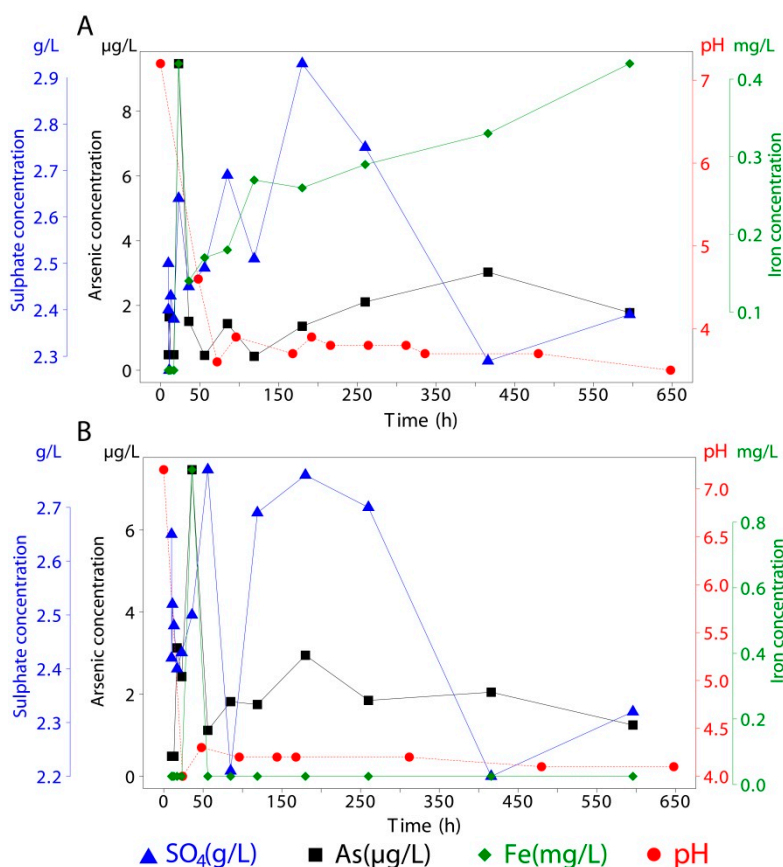
3.2. Arsenic Release from Schwertmannite

Arsenic release from schwertmannite with co-precipitated As remained at values close to normal seawater throughout the experiment ($\sim 2 \text{ µg/L}$), with the exception of up to 9 µg/L dissolved arsenic after 23 h, after this peak the value reduced again to normal seawater values within 13 h (Figure 5). An increase in iron and sulphate concentrations ($\text{Fe} > 0.4 \text{ mg/L}$ and $\text{SO}_4 > 2.6 \text{ g/L}$) showed consistency with arsenic liberation, which also decreased during the next hours, but at a slower rate than arsenic. During the first 72 h, pH dropped from seawater ($\text{pH} = 8.1$) to acidic values ($\text{pH} = 3.6$) confirming the high potential of schwertmannite to buffer the pH. Arsenic release after 23 h could indicate that

schwertmannite was able to dissolve or partially transform to a stable mineral while the circumneutral pH allowed it, however, due to the great charge difference between the environment and schwertmannite’s PZC, surface re-adsorption as well as co-precipitation processes were able to control ion release after it reached acid pH values.

Schwertmannite with adsorbed As in contact with seawater only released 7 µg/L of arsenic, within the first 36 h. The concentration then decreased to normal seawater values toward the end of the experiment, similarly to the previous case. At pH ~ 3.7, a slight increase in arsenic (7 µg/L), iron (0.96 mg/L), and sulphate (2.5 g/L) concentrations can be interpreted as a minor dissolution that ends when the system normalizes around pH 4. In order to understand the low TLC (~0.81 wt %) compared with values given in the literature (~10 wt %) [56,65], it should be considered that under the Regensburg method a quick precipitation process could affect the morphology of the grains and subsequently the development of surface area [54].

Figure 5. Arsenic release test for schwertmannite. (A) Arsenic release from co-precipitated schwertmannite and (B) arsenic release from adsorbed schwertmannite.



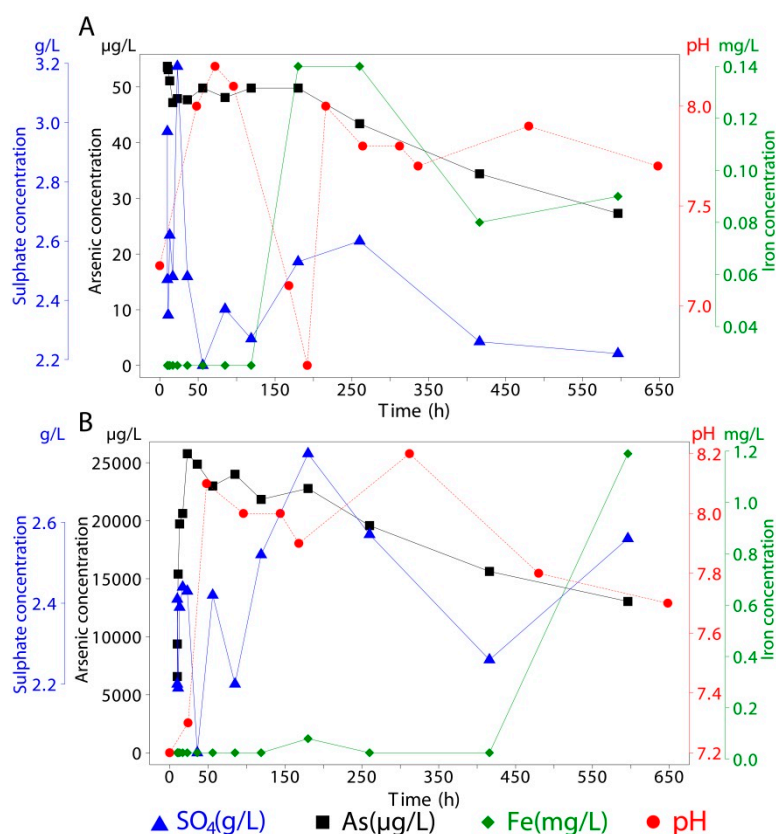
3.3. Arsenic Release from Goethite

The synthesis with co-precipitated As started with a release of 55 µg/L, which decreased to 27 µg/L after 586 h. From hour 50 to 180, a sustained decrease in pH from 8.2 to 6.7 set the start of Fe release, with a maximum of 0.14 mg/L that declined as pH stabilized at 7.8 by the end of the experiment (Figure 6). After 180 h, despite its high stability range, goethite released a significant amount of Fe that could be understood in terms of dissolution. When synthetic goethite presents short aging time, it

also can present a similar solubility product (K_{sp}) to ferrihydrite [66]. It is possible that given our synthesis conditions, a short aging time and a high K_{sp} , protonization over the goethite surface could be the responsible mechanism behind iron and arsenic release.

The synthesis with adsorbed As showed the greatest arsenic desorption by releasing 25.8 mg/L of arsenic at a rate of 1.43×10^{-5} mol/L/h during the first day in contact with seawater (Figure 6). The pH underwent multiple changes, going from normal seawater to pH 7.2 to 8.1 within the first 48 h. These trends also correlated with arsenic liberation. Iron continued below detection limit in almost every extraction and sulphate presented the lowest average levels for this mineral. PhreePlot computations for goethite surface complexes showed that above pH 8, soluble arsenic species predominate in a seawater environment, so natural arsenic release is expected at high pH. This occurs due to a lower stability in surface complexes as arsenic ions exchange with seawater species, mainly sulphate. At lower pH, re-adsorption would occur as $(OAsO_2OH^{-1.5})$ complexes that can result in a reduction of up to 50% of the initial release of dissolved arsenic by the end of the experiment.

Figure 6. Arsenic release test for goethite. (A) Arsenic release from co-precipitated goethite and (B) arsenic release from adsorbed goethite.



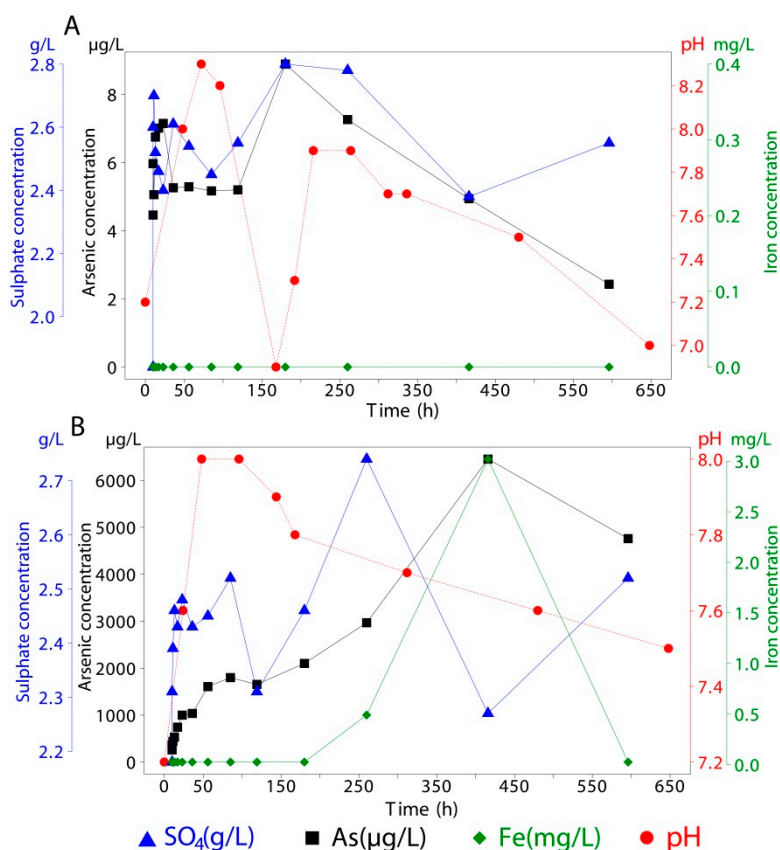
3.4. Arsenic Release from Jarosite

Among the studied minerals, jarosite with co-precipitated arsenic showed the lowest levels of uptake in adsorbed and co-precipitated synthesis. Arsenic release during contact with seawater was less than 9 $\mu\text{g/L}$, which represents about 0.15% of the TLC. Iron remained below the detection limit even though the stability field for jarosite is restricted to acid environments. Sulphate kept stable during the experiment. Considering theories that could explain the limited arsenic release, it is possible

that As co-precipitation caused a decrease in solubility [67] or release of sulphate caused precipitation of a Fe-OOH coating, protecting jarosite from the surrounding media [68].

Similarly to goethite, jarosite with adsorbed As showed high desorption by releasing up to 6452 µg/L, which corresponds to 45% TLC (Figure 7). The pH maintained around 7.6 but with variations within the first hours. After contact with seawater, the pH first decreased to 7.2 to thereafter increase to 8 at the same time that a large quantity of arsenic was released. A relationship between pH and desorption range can be observed. When the system reached pH 8, arsenic gradually increased in concentration, until pH dropped again. At this stage, the arsenic release began to occur at a higher rate. Given that there was no release of iron but sulphate remained at nominal values for seawater, it is possible that sulphate exchange could be taking place on the jarosite surface, promoting arsenic release. In this case, re-adsorption would not take place due to higher pH values [69].

Figure 7. Arsenic release test for jarosite. (A) Arsenic release from co-precipitated jarosite and (B) arsenic release from adsorbed jarosite.



4. Conclusions

During this laboratory study, some common Fe(III) hydroxides and oxyhydroxy-sulphates, including ferrihydrite, goethite, schwertmannite, and jarosite, present in the oxidation zone of mine tailings and in acid soils, showed efficacy as arsenic sorbents under several experimental conditions. Goethite and ferrihydrite were able to adsorb large loads of arsenic at their surfaces (~3 wt %) while schwertmannite and jarosite were able to incorporate less than 0.8 and 0.3 wt % of arsenic,

respectively. Once in contact with seawater, each mineral showed different sorbent capacities, depending on the type of arsenic load and mineral stability.

Our results demonstrated that during seawater intrusion in coastal tailings, arsenic release can be attributed mainly to ion exchange and dissolution processes. Ferrihydrite and schwertmannite, two meta-stable minerals with large reactive surface areas, were less likely to release arsenic due to a higher ZPC and schwertmannite's buffering capacity that acidified the pH of contact seawater. Moreover, highly stable goethite and jarosite showed the greatest release among minerals with adsorbed arsenic.

In general terms, synthesized minerals with co-precipitated arsenic were less inclined to liberation in comparison with syntheses with adsorbed arsenic, where ion exchange was a key parameter for liberation of the metalloid.

Schwertmannite and ferrihydrite presented the highest retention; however in the first case it mostly depended on the pH buffering capacity. It can be hypothesized that, under a real scale flooding scenario, schwertmannite would not be able to acidify the seawater in the same way it did in this experiment and that sea water geochemistry would dominate. In this case, a lower retention would be expected. In the medium term, transformation processes can release significant amounts of As that would not be fully retained by new sorbents. In the case of schwertmannite, exchange between sulphate and several species can affect stability and increase transformation rates to goethite [70]. The increase in dissolved iron and sulphate from schwertmannite towards the end of the experiment may indicate low stability or the beginning of transformation/dissolution processes. Ferrihydrite demonstrated its importance in coastal environments by representing a sink for arsenic at alkaline pH. However, the meta-stable nature for this mineral implies that in the long term dissolution and transformation processes can release arsenic regardless.

Goethite, another common stable mineral in the coastal environment, was not able to retain adsorbed arsenic after contact with seawater. This was due to the lower stability that surfaces complexes presented under seawater conditions. Although some authors have proposed bidentate complexes as the main linkage for arsenic in goethite's surface, in this case the release of 20% TLC would be more in accordance with less stable monodentate complexes as proposed by Loring [35].

In coastal environments, stability of sorbent minerals should be considered as a whole, taking into account interaction between sorbents, fate and transport of toxic elements, surface complexation, interaction with seawater species, transformation into stable minerals, and dissolution processes.

Acknowledgments

We acknowledge the Staff of the laboratory of the Institute for Applied Economic Geology (GEA) University of Concepcion, Chile for their support during experiment and analysis. We also gratefully acknowledges to Pierre Rousseau who helped us by reviewing this work.

Author Contributions

Experimental design, data collection, and analysis was conducted by Jenny Gaviria under the supervision of Bernhard Dold. Rodrigo Alarcón was in charge of data interpretation, analysis and scientific writing under the supervision of Bernhard Dold.

Conflicts of Interest

The authors declare no conflict of interest.

References

1. Zhao, Z.; Jia, Y.; Xu, L.; Zhao, S. Adsorption and heterogeneous oxidation of As(III) on ferrihydrite. *Water Res.* **2011**, *45*, 6496–6504.
2. Halim, M.A.; Majumder, R.K.; Nessa, S.A.; Hiroshiro, Y.; Uddin, M.J.; Shimada, J.; Jinno, K. Hydrogeochemistry and arsenic contamination of groundwater in the Ganges Delta Plain, Bangladesh. *J. Hazard. Mater.* **2009**, *164*, 1335–1345.
3. Anawar, H.M.; Akai, J.; Komaki, K.; Terao, H.; Yoshioka, T.; Ishizuka, T.; Safiullah, S.; Kato, K. Geochemical occurrence of arsenic in groundwater of Bangladesh: sources and mobilization processes. *J. Geochem. Explor.* **2003**, *77*, 109–131.
4. Kao, Y.H.; Wang, S.W.; Liu, C.W.; Wang, P.L.; Wang, C.H.; Maji, S.K. Biogeochemical cycling of arsenic in coastal salinized aquifers: Evidence from sulfur isotope study. *Sci. Total Environ.* **2011**, *409*, 4818–4830.
5. Jevrejeva, S.; Moore, J.; Grinsted, A. Sea level projections to AD2500 with a new generation of climate change scenarios. *Glob. Planet. Chang.* **2012**, *80–81*, 14–20.
6. Wang, S.; Mulligan, C.N. Natural attenuation processes for remediation of arsenic contaminated soils and groundwater. *J. Hazard. Mater.* **2006**, *138*, 459–470.
7. Mohan, D.; Pittman, C.U. Arsenic removal from water/wastewater using adsorbents—A critical review. *J. Hazard. Mater.* **2007**, *142*, 1–53.
8. Gao, Y.; Mucci, A. Individual and competitive adsorption of phosphate and arsenate on goethite in artificial seawater. *Chem. Geol.* **2003**, *199*, 91–109.
9. Zhang, H.; Selim, H.M. Kinetics of arsenate adsorption-desorption in soils. *Environ. Sci. Technol.* **2005**, *39*, 6101–6108.
10. Lakshmipathiraj, P.; Narasimhan, B.R.V.; Prabhakar, S.; Bhaskar Raju, G. Adsorption studies of arsenic on Mn-substituted iron oxyhydroxide. *J. Colloid Interface Sci.* **2006**, *304*, 317–322.
11. Luengo, C.; Brigante, M.; Avena, M. Adsorption kinetics of phosphate and arsenate on goethite. A comparative study. *J. Colloid Interface Sci.* **2007**, *311*, 354–360.
12. Mamindy-Pajany, Y.; Hurel, C.; Marmier, N.; Roméo, M. Arsenic adsorption onto hematite and goethite. *Comptes Rendus Chim.* **2009**, *12*, 876–881.
13. Dold, B.; Fontboté, L. Element cycling and secondary mineralogy in porphyry copper tailings as a function of climate, primary mineralogy, and mineral processing. *J. Geochem. Explor.* **2001**, *74*, 3–55.
14. Dold, B.; Diaby, N.; Spangenberg, J.E. Remediation of a marine shore tailings deposit and the importance of water-rock interaction on element cycling in the coastal aquifer. *Environ. Sci. Technol.* **2011**, *45*, 4876–4883.
15. Bigham, J.; Nordstrom, D.K. Iron and aluminum hydroxy- sulphates from acid sulphate waters. *Rev. Mineral. Geochem.* **2000**, *40*, 351–403.
16. Dold, B. Sustainability in metal mining: from exploration, over processing to mine waste management. *Rev. Environ. Sci. Biotechnol.* **2008**, *7*, 275–285.

17. Schwertmann, U.; Cornell, R.M. *Iron Oxides in Laboratory*, 2nd ed.; Wiley-VCH: Weinheim, Germany, 1993; pp. 5–110.
18. Cudennec, Y.; Lecerf, A. The transformation of ferrihydrite into goethite or hematite, revisited. *J. Solid State Chem.* **2006**, *179*, 716–722.
19. Bigham, J.M.; Schwertmann, U.; Traina, S.J.; Winland, R.L.; Wolf, M. Schwertmannite and the chemical modeling of iron in acid sulphate waters. *Geochim. Cosmochim.* **1996**, *60*, 2111–2121.
20. Caraballo, M.A.; Rimstidt, J.D.; Macías, F.; Nieto, J.M.; Hochella, M.F. Metastability, nanocrystallinity and pseudo-solid solution effects on the understanding of schwertmannite solubility. *Chem. Geol.* **2013**, *360–361*, 22–31.
21. Zinder, B.; Furrer, G.; Stumm, W. The coordination chemistry of weathering: II. Dissolution of Fe(III) oxides. *Geochim. Cosmochim.* **1986**, *50*, 1861–1869.
22. Stumm, W. *Chemistry of the Solid-Water Interface: Processes at the Mineral-Water and Particle-Water Interface in Natural Systems*, 1st ed.; John Wiley and Sons: New York, NY, USA, 1992; pp. 309–335.
23. Bennett, B.; Dudas, M.J. Release of arsenic and molybdenum by reductive dissolution of iron oxides in a soil with enriched levels of native arsenic. *J. Environ. Eng. Sci.* **2003**, *2*, 265–272.
24. Paktnuc, D. Mobilization of arsenic from mine tailings through reductive dissolution of goethite influenced by organic cover. *Appl. Geochem.* **2013**, *36*, 49–56.
25. Dutrizac, J.E.; Jambor, J.L. Jarosites and their application in hydrometallurgy. *Rev. Mineral. Geochem.* **2000**, *40*, 405–452.
26. Stoffregen, R.E.; Alpers, C.N.; Jambor, J.L. Alunite-jarosite crystallography, thermodynamics, and geochronology. *Rev. Mineral. Geochem.* **2000**, *40*, 453–479.
27. Fuller, C.C.; Davis, J.A.; Waychunas, G.A. Surface chemistry of ferrihydrite: Part 2. Kinetics of arsenate adsorption and coprecipitation. *Geochim. Cosmochim.* **1993**, *57*, 2271–2282.
28. Sun, X.; Doner, H.E. An investigation of arsenate and arsenite bonding structures on goethite by FTIR. *Soil Sci.* **1996**, *161*, 865–872.
29. Goldberg, S.; Johnston, C.T. Mechanisms of arsenic adsorption on amorphous oxides evaluated using macroscopic measurements, vibrational spectroscopy, and surface complexation modeling. *J. Colloid Interface Sci.* **2001**, *234*, 204–216.
30. Waychunas, G.A.; Rea, B.A.; Fuller, C.C.; Davis, J.A. Surface chemistry of ferrihydrite: Part 1. EXAFS studies of the geometry of coprecipitated and adsorbed arsenate. *Geochim. Cosmochim. Acta* **1993**, *57*, 2251–2269.
31. Sherman, D.M.; Randall, S.R. Surface complexation of arsenic(V) to iron(III) (hydr)oxides: structural mechanism from *ab initio* molecular geometries and EXAFS spectroscopy. *Geochim. Cosmochim.* **2003**, *67*, 4223–4230.
32. Stachowicz, M.; Hiemstra, T.; Van Riemsdijk, W.H. Surface speciation of As(III) and As(V) in relation to charge distribution. *J. Colloid Interface Sci.* **2006**, *302*, 62–75.
33. Manceau, A. The mechanism of anion adsorption on iron oxides: Evidence for the bonding of arsenate tetrahedra on free Fe(O, OH)₆ edges. *Geochim. Cosmochim.* **1995**, *59*, 3647–3653.
34. Paktunc, D.; Foster, A.; Heald, S.; Laflamme, G. Speciation and characterization of arsenic in gold ores and cyanidation tailings using X-ray absorption spectroscopy. *Geochim. Cosmochim.* **2004**, *68*, 969–983.

35. Loring, J.S.; Sandström, M.H.; Norén, K.; Persson, P. Rethinking arsenate coordination at the surface of goethite. *Chem. Eur. J.* **2009**, *15*, 5063–5072.
36. Guan, X.H.; Wang, J.; Chusuei, C.C. Removal of arsenic from water using granular ferric hydroxide: macroscopic and microscopic studies. *J. Hazard. Mater.* **2008**, *156*, 178–185.
37. Zhu, J.; Pigna, M.; Cozzolino, V.; Caporale, A.G.; Violante, A. Sorption of arsenite and arsenate on ferrihydrite: Effect of organic and inorganic ligands. *J. Hazard. Mater.* **2011**, *189*, 564–571.
38. Su, C.; Puls, R. Arsenate and arsenite removal by zerovalent iron: Effects of phosphate, silicate, carbonate, borate, sulphate, chromate, molybdate, and nitrate, relative to chloride. *Environ. Sci. Technol.* **2001**, *35*, 4562–4568.
39. Stuckman, M.Y.; Lenhart, J.J.; Walker, H.W. Abiotic properties of landfill leachate controlling arsenic release from drinking water adsorbents. *Water Res.* **2011**, *45*, 4782–4792.
40. Dold, B. Submarine tailings disposal (STD)—A review. *Minerals* **2014**, *4*, 642–666.
41. Brewer, D.T.; Morello, E.B.; Griffiths, S.; Fry, G.; Heales, D.; Apte, S.C.; Venables, W.N.; Rothlisberg, P.C.; Moeseneder, C.; Lansdell, M.; Pendrey, R.; Coman, F.; Strzelecki, J.; Jarolimek, C.V.; Jung, R.F.; Richardson, A.J. Impacts of gold mine waste disposal on a tropical pelagic ecosystem. *Mar. Pollut. Bull.* **2012**, *64*, 2790–2806.
42. Ellis, D.V.; Poling, G.W.; Baer, R.L. Submarine tailings disposal (STD) for mines: An introduction. *Mar. Georesour. Geotechnol.* **1995**, *13*, 3–18.
43. Dold, B. Element flows associated with marine shore mine tailings deposits. *Environ. Sci. Technol.* **2006**, *40*, 752–758.
44. Lee, M.R.; Correa, J.A. Effects of copper mine tailings disposal on littoral meiofaunal assemblages in the Atacama region of northern Chile. *Mar. Environ. Res.* **2005**, *59*, 1–18.
45. Lee, M.R.; Correa, J.A.; Seed, R. A sediment quality triad assessment of the impact of copper mine tailings disposal on the littoral sedimentary environment in the Atacama region of northern Chile. *Mar. Pollut. Bull.* **2006**, *52*, 1389–1395.
46. Bea, S.A.; Ayora, C.; Carrera, J.; Saaltink, M.W.; Dold, B. Geochemical and environmental controls on the genesis of soluble efflorescent salts in Coastal Mine Tailings Deposits: A discussion based on reactive transport modeling. *J. Contam. Hydrol.* **2010**, *111*, 65–82.
47. Sharma, V.K.; Sohn, M. Aquatic arsenic: toxicity, speciation, transformations, and remediation. *Environ. Int.* **2009**, *35*, 743–759.
48. Yusof, A.M.; Ikhsan, Z.B.; Wood, A. The speciation of arsenic in seawater and marine species. *J. Radioanal. Nucl. Chem.* **1994**, *179*, 277–283.
49. Maher, W.; Butler, E. Arsenic in the marine environment. *Appl. Organomet. Chem.* **1988**, *2*, 191–214.
50. Ogawa, H.; Tanoue, E. Dissolved organic matter in oceanic waters. *J. Oceanogr.* **2003**, *59*, 129–147.
51. Rose, A.L.; Waite, T. Kinetics of iron complexation by dissolved natural organic matter in coastal waters. *Mar. Chem.* **2003**, *84*, 85–103.
52. Dold, B.; Fontboté, L. A mineralogical and geochemical study of element mobility in sulphide mine tailings of Fe oxide Cu–Au deposits from the Punta del Cobre belt, northern Chile. *Chem. Geol.* **2002**, *189*, 135–163.
53. Regenspurg, S.; Brand, A.; Peiffer, S. Formation and stability of schwertmannite in acidic mining lakes 1. *Geochim. Cosmochim.* **2004**, *68*, 1185–1197.

54. Baron, D.; Palmer, C.D. Solubility of $\text{KFe}_3(\text{CrO}_4)_2(\text{OH})_6$ at 4 to 35 °C. *Geochim. Cosmochim.* **1996**, *60*, 3815–3824.
55. Drouet, C.; Navrotsky, A. Synthesis, characterization, and thermochemistry of K-Na- H_3O jarosites. *Geochim. Cosmochim.* **2003**, *67*, 2063–2076.
56. Dutrizac, J. The behaviour of the rare earths during the precipitation of sodium, potassium and lead jarosites. *Hydrometallurgy* **2004**, *73*, 11–30.
57. Cornell, R.; Schwertmann, U. *The Iron Oxides: Structure, Properties, Reactions, Occurrences and Uses*, 2nd ed.; Wiley-VCH: Weinheim, Germany, **2003**; pp. 9–37.
58. Acero, P.; Ayora, C.; Torrento, C.; Nieto, J. The behavior of trace elements during schwertmannite precipitation and subsequent transformation into goethite and jarosite. *Geochim. Cosmochim.* **2006**, *70*, 4130–4139.
59. Strawn, D.G.; Sparks, D.L. Residence time effects on arsenate adsorption/desorption mechanisms on goethite. *Soil Sci. Soc. Am.* **2001**, *65*, 67–77.
60. PhreePlot. Available online: <http://www.phreeplot.org/> (accessed on 1 February 2014).
61. Nordstrom, D.; Plummer, L.; Wigley, T.; Wolrey, T.; Ball, J. A Comparison of Computerized Chemical Models for Equilibrium Calculations in Aqueous Systems. In *Chemical Modeling in Aqueous Systems*, 1st ed.; Jenne, E.A., Ed.; American Chemical Society: Washington, DC, USA, 1979; Volume 1, pp. 875–892.
62. Turekian, K.K. *Oceans*; Prentice-Hall: Upper Saddle River, NJ, USA, 1976.
63. Jain, A.; Raven, K.P.; Loeppert, R.H. Arsenite and arsenate adsorption on ferrihydrite: Surface charge reduction and net OH^- release stoichiometry. *Environ. Sci. Technol.* **1999**, *33*, 1179–1184.
64. Das, S.; Hendry, M.J.; Essilfie-Dughan, J. Transformation of two-line ferrihydrite to goethite and hematite as a function of pH and temperature. *Environ. Sci. Technol.* **2011**, *45*, 268–275.
65. Subrt, J.; Bohacek, J.; Stengl, V.; Grygar, T.; Bezdicka, P. Uniform particles with a large surface area formed by hydrolysis of $\text{Fe}_2(\text{SO}_4)_3$ with urea. *Mater. Res. Bull.* **1999**, *34*, 905–914.
66. Schwertmann, U.; Miinchen, T.U. Solubility and dissolution of iron oxides. *Plant Soil.* **1991**, *130*, 1–25.
67. Savage, K.S.; Bird, D.K.; O’Day, P.A. Arsenic speciation in synthetic jarosite. *Chem. Geol.* **2005**, *215*, 473–498.
68. Welch, S.A.; Kirste, D.; Christy, A.G.; Beavis, F.R.; Beavis, S.G. Jarosite dissolution II- Reaction kinetics, stoichiometry and acid flux. *Chem. Geol.* **2008**, *254*, 73–86.
69. Zygmunt, S.; Polowczyk, I.; Farbiszewska, T.; Farbiszewska-Kiczma, J. Adhesion of jarosite particles to the mineral surface. *Prace Naukowe Instytutu Górnicztwa Politechniki Wrocławskiej* **2001**, *95*, 95–103.
70. Antelo, J.; Fiol, S.; Gondar, D.; López, R.; Arce, F. Comparison of arsenate, chromate and molybdate binding on schwertmannite: Surface adsorption vs anion-exchange. *J. Colloid Interface Sci.* **2012**, *386*, 338–343.